Chinese Chemical Letters 32 (2021) 1721–1725

Contents lists available at ScienceDirect

Chinese Chemical Letters

journal homepage: www.elsevier.com/locate/cclet

Communication

# Psiguamers A–C, three cytotoxic meroterpenoids bearing a methylated benzoylphloroglucinol framework from *Psidium guajava* and total synthesis of **1** and **2**

Jiwu Huang, Chuangjun Li, Jie Ma, Yingda Zang, Xingyan Sun, Xiaoguang Chen, Dongming Zhang*

*State Key Laboratory of Bioactive Substance and Function of Natural Medicines, Institute of Materia Medica, Chinese Academy of Medical Sciences and Peking Union Medical College, Beijing 100050, China*

ARTICLE INFO

*Article history:*
Received 27 August 2020
Received in revised form 27 September 2020
Accepted 12 November 2020
Available online 22 November 2020

*Keywords:*
*Psidium guajava*
Methylated benzoylphloroglucinol
Meroterpenoids
Biomimetic synthesis
Cytotoxic activities

ABSTRACT

Three sesquiterpene-based meroterpenoids psiguamers A–C (**1**–**3**) with new skeletons were isolated from *Psidium guajava* leaves. Compounds (±)-**1** and (±)-**2** were two pairs of humulene-derived meroterpenoids bearing a rare methylated benzoylphloroglucinol unit, while **3** was an unprecedented adduct of bicyclogermacrene and methylated benzoylphloroglucinol. Their structures were determined based on comprehensive analyses of spectroscopic data, calculated electronic circular dichroism (ECD) spectra, total synthesis, and X-ray crystallographic data. The biomimetic synthesis of (±)-**1** and (±)-**2** was achieved. Compound (+)-**1** exhibited cytotoxic activities against five human tumor cell lines (HCT-116, HepG2, BGC-823, A549, and U251), with $IC_{50}$ values of 2.94, 9.01, 6.45, 5.42, and 5.33 μmol/L, respectively.



*Psidium* meroterpenoids, a group of intricate molecules that are part terpenoids, part natural phloroglucinol, possess a wide range of interesting bioactivities. Modern pharmacological investigations showed meroterpenoids from *P. guajava* leaves exhibited significant bioactivity, such as hepatoprotective, anti-inflammatory, anticancer, and protein tyrosine phosphatase 1B (PTP1B) inhibitory activity [1–4]. Structurally, according to the phenolic moiety, *Psidium* meroterpenoids can be classified as two groups, formyl-benzyl phloroglucinol and methylated benzoylphloroglucinol types [5,6]. Among these meroterpenoids, most of them are caryophyllane or cadinane derived meroterpenoids with a 3,5-diformyl-benzyl phloroglucinol unit [7–9]. However, methylated benzoylphloroglucinol meroterpenoids were rarely reported, and only caryophyllane type was found since 2015 [2,5,6]. Herein, we first report humulene and bicyclogermacrene derived methylated benzoylphloroglucinol meroterpenoids from the leaves of *Psidium guajava*. Compounds (±)-**1** and (±)-**2** were two pairs of unprecedented humulene derived meroterpenoids with a 6/6/11 ring system, and **3** was an unusual bicyclogermacrene derived meroterpenoid with a 6/6/10/3 ring framework (Fig. 1). Moreover, the total synthesis of (±)-psiguamer A (**1**) and (±)-psiguamer B (**2**) was achieved, and all the isolates were evaluated for their cytotoxicity.

(±)-Psiguamer A (**1**) was obtained as a white amorphous powder with the molecular formula $C_{30}H_{34}O_5$, determined by the (−)-HRESIMS ion peak at *m/z* of 473.2335 $[M-H]^-$ (Calcd. for 473.2334) with an index of hydrogen deficiency of 14. The $^1$H NMR data (Table 1) showed two hydrogen-bonded phenolic hydroxyls ($\delta_H$ 13.72 (s, 1H) and 13.28 (s, 1H)), an aldehyde group ($\delta_H$ 10.25 (s, 1H)), a monosubstituted benzene ring ($\delta_H$ 7.37–7.45 (5H)), three alkene protons ($\delta_H$ 4.95 (dd, *J* = 4.2, 12.0 Hz, 1H), 4.92 (d, *J* = 15.6 Hz, 1H), and 4.56 (ddd, *J* = 2.4, 10.8, 15.6 Hz, 1H)) and four methyl groups ($\delta_H$ 1.55, 1.01, 0.99, and 0.92 (each, s, 3H)). The $^{13}$C NMR and DEPT spectra presented a total of 30 carbon signals, including a ketone carbonyl ($\delta_C$ 200.4), a conjugated aldehyde ($\delta_C$ 192.2), a hexasubstituted benzene ring ($\delta_C$ 168.8, 167.3, 162.3, 104.3, 103.8, and 100.8), a monosubstituted benzene ring (($\delta_C$ 142.5, 130.2, 127.9 (×2), and 126.5 (×2)), four olefinic carbons ($\delta_C$ 142.4, 136.4, 123.1, and 119.9), four methyl ($\delta_C$ 30.2, 24.4, 19.8, and 17.1), five methylene ($\delta_C$ 41.7, 41.3, 37.5, 30.1, and 22.0), one methine, one quaternary, and one oxygenated tertiary carbons. The above data indicated that **1** was a sesquiterpene-based meroterpenoid.

The $^1$H-$^1$H COSY spectrum (Fig. 2A) showed cross peaks for H-1/H-2/H-3, H-1′/H-5/H-6/H-7, and H-9/H-10 coupling systems.

* Corresponding author.
*E-mail address:* zhangdm@imm.ac.cn (D. Zhang).

https://doi.org/10.1016/j.cclet.2020.11.028

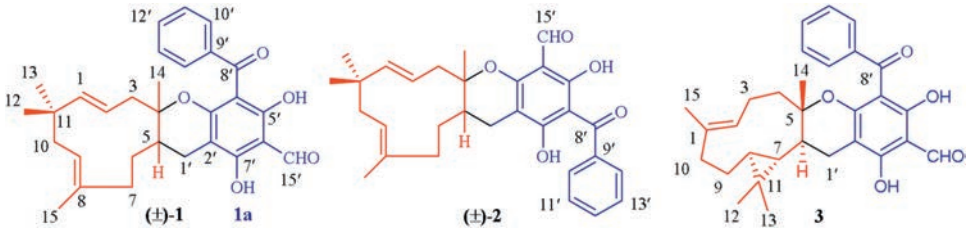


**Fig. 1.** Chemical structures of compounds **1**–**3**.

The HMBC spectrum (Fig. 2A) revealed correlations from $H_3$-12 to C-1, C-10, and C-13, from $H_3$-13 to C-1, C-10, and C-12, from $H_3$-14 to C-3 and C-5, and from $H_3$-15 to C-7 and C-9, indicating the presence of a humulene moiety. Similarly, the presence of 3-methyl-5-formyl-benzoyl phloroglucinol unit (**1a**) was determined by a series of HMBC cross signals from H-1′ to C-3′ and C-7′, from H-10′ and H-14′ to C-8′, from H-5′-OH to C-4′ and C-6′, from H-7′-OH to C-2′ and C-6′, and from H-15′ to C-6′. The humulene moiety and **1a** were linked through the C-5–C-1′ bond, as indicated by HMBC correlations from H-1′ to C-4 and C-6, and from H-6 to C-1′. Moreover, the oxygenated tertiary carbon C-4 ($\delta_C$ 84.8) and the downfield chemical shift of C-3′ ($\delta_C$ 162.3) connecting with an index of hydrogen deficiency of 14 demonstrated that a dihydropyran ring connecting the humulene moiety and **1a**.

The relative configuration of **1** was determined by its rotating-frame overhauser spectroscopy (ROESY) NMR spectrum (Fig. 2A) and proton coupling constants. The ROESY correlations between H-1 and H-3a, between H-2 and $H_3$-13 revealed the *E*-geometry of the C1/C2 double-bond, which was consistent with the large coupling constant that was observed ($J_{H1-2}$ = 15.6 Hz). The *E*-geometry of the C8/C9 olefin was determined by the ROESY correlations between H-9 and H-7b, between $H_3$-15 and H-10a. Furthermore, ROESY correlations between H-2 and H-5, between H-5 and H-9, and between H-9 and H-2 demonstrated that H-2, H-5, and H-9 were on the same side of the molecule, while H-1 and $H_3$-15 were on the opposite side. Two peaks were found in the chiral HPLC analysis of **1**, indicating that **1** was a racemic mixture. Consequently, a cellulose-4 chiral column was used to separate **1**

**Table 1**
$^1$H NMR (600 MHz) and $^{13}$C NMR (150 MHz) spectroscopic data for compounds **1**–**3** ($\delta$ in ppm, $CDCl_3$).

| No. | **1** | | **2** | | **3** | |
|---|---|---|---|---|---|---|
| | $\delta_C$ | $\delta_H$ (*J*, Hz) | $\delta_C$ | $\delta_H$ (*J*, Hz) | $\delta_C$ | $\delta_H$ (*J*, Hz) |
| 1 | 142.2 | 4.92 d (15.6) | 143.4 | 5.18 dd (16.2, 1.8) | 131.7 | |
| 2 | 119.9 | 4.56 ddd (15.6, 10.8, 2.4) | 119.5 | 5.05[a] | 127.3 | 5.08 dd (11.4, 3.0) |
| 3a | 41.7 | 1.87 dd (14.4, 10.8) | 42.5 | 2.63 d (14.4) | 22.0 | 1.61 m |
| 3b | | 1.34 d (14.4) | | 2.37 dd (14.4, 10.8) | | 1.38 m |
| 4a | 84.8 | | 84.5 | | 38.3 | 1.52 t (1.8) |
| 4b | | | | | | 0.85 m |
| 5 | 34.1 | 1.62 m | 34.8 | 1.87 m | 85.2 | |
| 6a | 30.1 | 1.12 m | 30.2 | 1.34 m | 33.2 | 1.63 m |
| 6b | | 1.12 m | | 1.23 m | | |
| 7a | 37.5 | 2.06 dd (12.6, 7.2) | 37.7 | 2.14 dd (12.6, 7.2) | 28.2 | 0.14 dd (9.0, 5.4) |
| 7b | | 1.80 t (12.0) | | 1.89 m | | |
| 8 | 136.4 | | 136.5 | | 29.5 | 0.39 m |
| 9a | 123.1 | 4.95 dd (12.0, 4.2) | 123.2 | 5.05[a] | 23.4 | 1.77 m |
| 9b | | | | | | 0.83 m |
| 10a | 41.3 | 2.12 t (12.0) | 41.5 | 2.20 t (12.6) | 38.1 | 2.04 m |
| 10b | | 1.72 dd (13.2, 4.2) | | 1.72 dd (12.6, 4.2) | | 1.89 td (12.6, 2.4) |
| 11 | 38.1 | | 38.3 | | 18.3 | |
| 12 | 24.4 | 0.99 s | 24.4 | 1.04 s | 18.5 | 1.11 s |
| 13 | 30.2 | 1.01 s | 30.2 | 1.07 s | 31.3 | 1.05 s |
| 14 | 19.8 | 0.92 s | 20.4 | 1.21 s | 20.5 | 1.06 s |
| 15 | 17.1 | 1.55 s | 17.2 | 1.64 s | 17.8 | 1.50 s |
| 1′a | 22.0 | 2.95 dd (16.8, 5.4) | 22.4 | 3.05 dd (16.8, 5.4) | 22.3 | 2.76 dd (16.8, 6.0) |
| 1′b | | 1.96 dd (16.8, 12.6) | | 2.08 dd (16.8, 12.0) | | 2.16 m |
| 2′ | 100.8 | | 101.3 | | 101.8 | |
| 3′ | 162.3 | | 162.2 | | 162.3 | |
| 4′ | 103.8 | | 104.1 | | 103.9 | |
| 5′ | 168.8 | | 166.8 | | 168.7 | |
| 6′ | 104.3 | | 102.9 | | 104.3 | |
| 7′ | 167.3 | | 169.4 | | 167.6 | |
| 8′ | 200.4 | | 199.7 | | 200.4 | |
| 9′ | 142.5 | | 140.8 | | 142.7 | |
| 10′ | 127.9 | 7.40 m | 128.1 | 7.63 m | 127.9 | 7.42 m |
| 11′ | 126.5 | 7.37 m | 127.8 | 7.42 t (7.2) | 126.5 | 7.42 m |
| 12′ | 130.2 | 7.45 m | 131.5 | 7.52 t (7.2) | 130.2 | 7.47 m |
| 13′ | 126.5 | 7.37 m | 127.8 | 7.42 t (7.2) | 126.5 | 7.42 m |
| 14′ | 127.9 | 7.40 m | 128.1 | 7.63 m | 127.9 | 7.42 m |
| 15′ | 192.2 | 10.25 s | 191.8 | 10.03 s | 192.2 | 10.24 s |
| 5′-OH | | 13.72 s | | 13.66 s | | 13.66 s |
| 7′-OH | | 13.28 s | | 13.74 s | | 13.23 s |

[a] Overlapped.

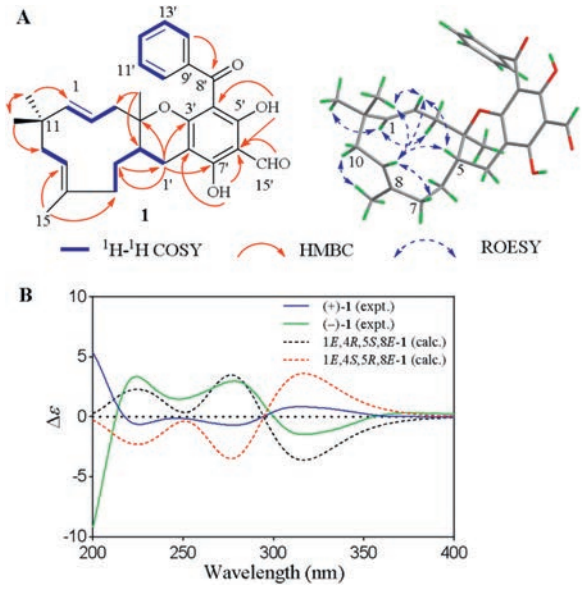


**Fig. 2.** (A) Selected 2D correlations of **1**. (B) Experimental and calculated ECD spectra of (+)-**1** and (–)-**1**.

and afforded (+)-**1** and (–)-**1**. Their absolute configurations were determined by comprehensive analysis of the experimental and calculated electronic circular dichroism (ECD) spectra (Fig. 2B) of **1**. The experimental ECD spectra of (+)-**1** and (–)-**1** were high consistent with the computed ECD data of 1*E*,4*S*,5*R*,8*E*-**1** and 1*E*,4*R*,5*S*,8*E*-**1**, respectively. Thus, (+)-psiguamer A [(+)-**1**] and (–)-psiguamer A [(–)-**1**] were established.

(±)-Psiguamer B (**2**) was isolated as a white amorphous powder with a molecular formula $C_{30}H_{34}O_5$, as determined by 1D NMR and the (+)-HRESIMS ion peak at *m/z* of 475.2481 $[M+H]^+$ (Calcd. for $C_{30}H_{35}O_5$ at 475.2479). Comparing its $^{13}$C NMR data with those of (±)-psiguamer A (**1**) revealed that compound **2** was an isomer of **1**, only differing at C-5′ ($\delta_C$ 166.8 in **2**, 168.8 in **1**), C-6′ ($\delta_C$ 102.9 in **2**, 104.3 in **1**), C-7′ ($\delta_C$ 169.4 in **2**, 167.3 in **1**), and C-9′ ($\delta_C$ 140.8 in **2**, 142.5 in **1**), indicating the location of phenyl unit of **2** was not the same as that of **1**. The position of phenyl ring was assigned by HMBC spectrum (Fig. S2.9 in Supporting information), in which H-10′ was correlated with C-8′, H-15′ with C-4′ and C-5′, H-5′-OH with C-4′ and C-6′, and H-7′-OH with C-2′ and C-6′. The relative configuration of **2** was established by the NOESY NMR spectrum (Fig. S2.10 in Supporting information). Two peaks were observed in the chiral HPLC analysis of **2**, suggesting that **2** was a racemic mixture, which was applied to a cellulose-4 chiral column to yield (+)-**2** and (–)-**2**.

The absolute configurations of (+)-**2** and (–)-**2** were established *via* ECD calculation. Compound 1*E*,4*S*,5*R*,8*E*-**2** was selected for the conformational analysis *via* Conflex 8B software at the MMF94S force field. The two lowest-energy conformers **2A** and **2B** (Fig. S2.11 in Supporting information) were selected for optimization with the TDDFT method at the B3LYP/6-31 G level in $CH_3CN$ with the CPCM (conductor-like polarizable continuum model) using the Gaussian 16 program. Due to the flexibility of the semi-chiral axis (C6′C8′), conformers **2A** and **2B** differed in the orientation of the monosubstituted benzene ring, which was consistent with the previously report [5]. Furthermore, a Boltzmann weight of approximately 1:1 for **2A** and **2B** led to a total cancellation between $\pi\rightarrow\pi^*$ and $n\rightarrow\pi^*$ transitions of **1a**. Thus, the overall computed ECD spectrum of **2** demonstrated minor Cotton effects (CEs) at 240–400 nm. However, the calculated ECD spectra of **2A** and **2B** presented similar CEs at approximately 211 nm (produced by the $\pi\rightarrow\pi^*$ transition of $\Delta^{1(2)}$), which contributed to an overall positive signal. Therefore, the stereo configuration of (+)-**2** can be established by comparing the CEs of the experimental ECD at 211 nm with calculated ECD. The experimental ECD of (+)-**2** (Fig. S2.12 in Supporting information) qualitatively matches the computed ECD spectrum of 1*E*,4*S*,5*R*,8*E*-**2**, suggesting that the steroconfiguration of (+)-psiguamer B [(+)-**2**] is 1*E*,4*S*,5*R*,8*E*. The absolute configuration of (–)-psiguamer B [(–)-**2**] was similarly established as 1*E*,4*R*,5*S*,8*E*.

Psiguamer C (**3**), colorless oil, had a molecular formula of $C_{30}H_{34}O_5$ based on its (+)-HRESIMS ion peak at *m/z* of 497.2304 $[M + Na]^+$ (Calcd. for $C_{30}H_{34}O_5Na$, 497.2298). Detailed comparison of

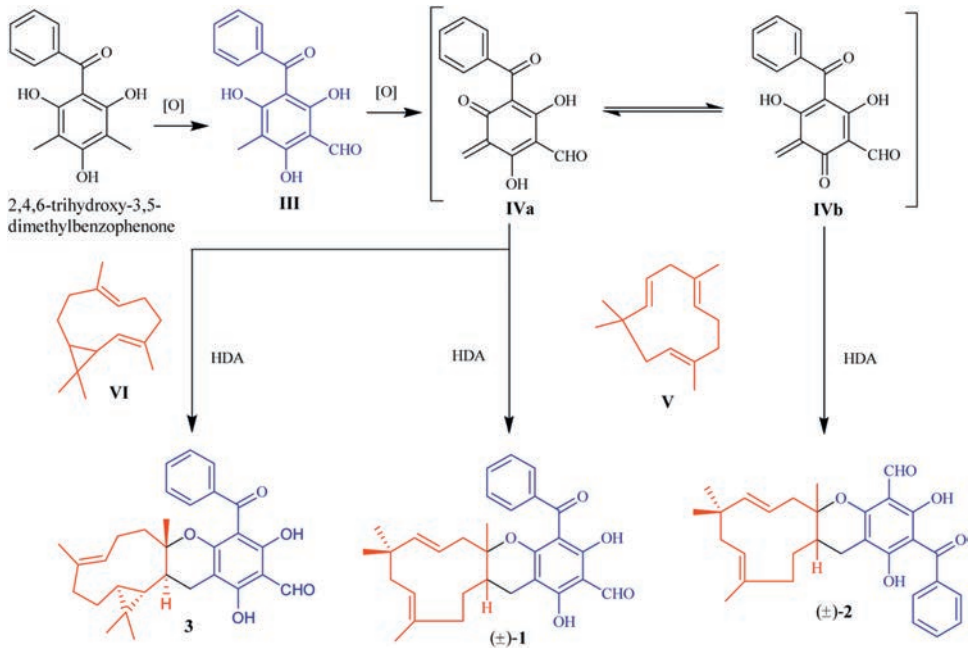


**Scheme 1.** Proposed biosynthetic pathway of compounds **1**–**3**.

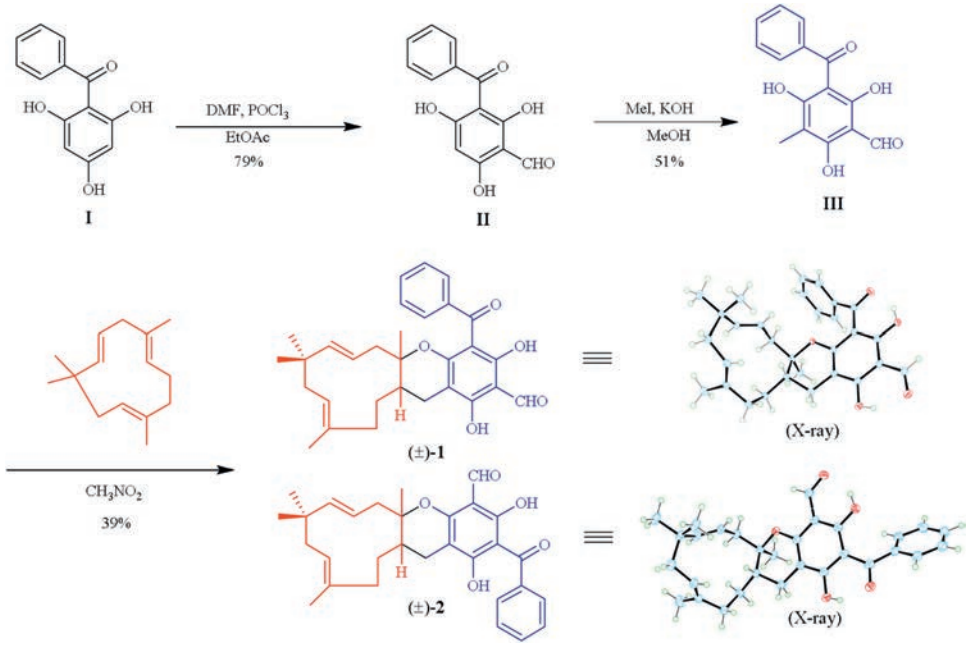


**Scheme 2.** Synthesis of (±)-psiguamers A (**1**) and B (**2**).

its $^{1}H$ and $^{13}C$ NMR data with those of literatures suggested compound **3** was an adduct of **1a** and a germacrene moiety as eucalteretial A [10]. In $^{1}H$-$^{1}H$ COSY spectrum (Fig. S3.7 in Supporting information), correlation between H-6 and H-1′ suggested a C-6–C-1′ coupling pattern in **3**, which was further confirmed by HMBC correlations from H-14 to C-6, from H-6 to C-1′ and C-2′, and from H-1′ to C-5, C-7, and C-3′ (Fig. S3.9 in Supporting information). The NOESY correlations (Fig. S3.10 in Supporting information) between $H_3$-15 and H-3b, between H-2 and H-10b suggested that an *E*-geometry of the C1/C2 olefin. The NOESY correlations of H-7/H-8, H-7/$H_3$-14, and $H_3$-14/H-1′ suggested these protons were co-facial. Finally, the absolute configuration of **3** was established as 1*E*,5*S*,6*S*,7*R*,8*S* by comparing the experimental and calculated ECD spectra (Fig. S3.11 in Supporting information).

Biosynthetic pathways for compounds **1**–**3** are proposed in Scheme 1. 2,4,6-Trihydroxy-3,5-dimethylbenzophenone, $\alpha$-humulene (**V**), and bicyclogermacrene (**VI**) were isolated from the *P. guajava* leaves [11–13]. Intermediate 2,4,6-trihydroxy-3,5-dimethylbenzophenone generates **III** under oxidation conditions, followed by the conversion of **III** to **IVa**, which is then tautomerized to **IVb** [2,14]. The resulting intermediates, **IVa** and **IVb** react with **V** *via* a HDA (hetero-Diels-Alder) reaction to yield **1** and **2**, respectively. Furthermore, under a HDA reaction with **VI**, **IVa** produces compound **3**.

To further confirmation of their structures, we have synthesized compounds **1** and **2** starting from commercially available 2-benzoylphloroglucinol (**I**) (Scheme 2). Inspired by Bharate and co-authors [15], 3-benzoyl-2,4,6-trihydroxy-benzaldehyde (**II**) was obtained in 79% yield by the formylation of **I**. Methylation, using methyl iodide and potassium hydroxide, provided 3-benzoyl-2,4,6-trihydroxy-5-methybenzaldehyde (**III**) in a 51% yield. With compound **III** in hand, the synthesis of compounds **1** and **2** *via* a HAD reaction was attempted by the mixing **III** with $\alpha$-humulene and DDQ (2,3-dichloro-5,6-dicyano-1,4-benzoquinone) in nitromethane to obtain (±)-psiguamers A (**1**) and B (**2**) as a 7:5 mixture with a 39% combined yield. Compounds **1** and **2** were definitively identified by X-ray crystallographic data (Fig. S4.13 for **1**, and Fig. S4.14 for **2**, Supporting information).

The cytotoxicity test of psiguamers A–C (**1**–**3**) in tumor cells was assessed by the MTT method [16]. As shown in Table S3 (Supporting information), compound (+)-**1** showed cytotoxic activities against five human tumor cell lines (HCT-116, HepG2, BGC-823, A549, and U251), with $IC_{50}$ values of 2.94, 9.01, 6.45, 5.42, and 5.33 μmol/L, respectively. Compound (+)-**2** was active against HCT-116 with $IC_{50}$ value of 2.25 μmol/L, while (−)-**2** exhibited cytotoxicity against HCT-116 and U251 with $IC_{50}$ values of 2.23 and 8.21 μmol/L, respectively. Unluckily, compounds (−)-**1** and (+)-**3** were inactive in cytotoxic assay. These results indicated that the absolute configurations of C-4 and C-5 played an important role in the cytotoxic activity.

In conclusion, psiguamers A–C (**1**–**3**) isolated from *P. guajava* leaves have been found to have unprecedented skeletons, a rare methylated benzoylphloroglucinol unit fusing with a humulene or a bicyclogermacrene fragment. These molecules could enrich the chemical diversity of methylated benzoylphloroglucinol derivatives. A biomimetic synthetic strategy for **1** and **2** was developed, and their structures were further confirmed by X-ray crystallographic data. Among these compounds, (+)-**1**, (+)-**2**, and (−)-**2** exhibited antitumor activity.

## Declaration of competing interest

The authors declare that they have no known competing financial interests or personal relationships that could have appeared to influence the work reported in this paper.

## Acknowledgments

This work was supported by the National Natural Science Foundation of China (No. 21772234), the National New Drug Innovation Major Project of China (Nos. 2018ZX09735006 and 2018ZX09711001-002-010), CAMS Innovation Fund for Medical Sciences (Nos. 2016-I2M-2-003 and 2017-I2M-3-010), and the independent project of State Key Laboratory of Bioactive Substance and Function of Natural Medicines (No. GTZA201803).

## Appendix A. Supplementary data

Supplementary material related to this article can be found, in the online version, at doi:https://doi.org/10.1016/j.cclet.2020.11.028.

## References

[1] H.Z. Fu, Y.M. Luo, C.J. Li, et al., Org. Lett. 12 (2010) 656–659.
[2] S. Ning, Z.L. Liu, Z.C. Wang, et al., Org. Lett. 21 (2019) 8700–8704.
[3] C.J. Li, J. Ma, H. Sun, et al., Org. Lett. 18 (2016) 168–171.
[4] X.J. Qin, Q. Yu, H. Yan, et al., J. Agric. Food Chem. 65 (2017) 4993–4999.
[5] Y.Q. Jian, X.J. Huang, D.M. Zhang, et al., Chem. Eur. J. 21 (2015) 9022–9027.
[6] G.H. Tang, Z. Dong, Y.Q. Guo, et al., Sci. Rep. 7 (2017) 1047.
[7] X.L. Yang, K.L. Hsieh, J.K. Liu, Org. Lett. 9 (2007) 5135–5138.
[8] Y. Gao, G.T. Li, Y. Li, et al., Nat. Prod. Bioprospect. 3 (2013) 14–19.
[9] J. Liu, L.R. Jiang, M.F. Liu, Chem. Nat. Compd. 52 (2016) 67–70.
[10] H. Liu, M.Y. Feng, Q. Yu, et al., Tetrahedron 74 (2018) 1540–1545.
[11] K.F. do Nascimento, F.M.F. Moreira, J.A. Santos, et al., J. Ethnopharmacol. 210 (2018) 351–358.
[12] G.E. Moussa, Acta Chem. Scand. 22 (1968) 3329–3330.
[13] T.D. de Souza, M.F. Ferreira, L. Menini, et al., Sci. Hortic. 216 (2017) 38–44.
[14] M. Shao, Y. Wang, Y.Q. Jian, et al., Org. Lett. 14 (2012) 5262–5265.
[15] S.B. Bharate, K.K. Bhutani, S.I. Khan, et al., Biorg. Med. Chem. 14 (2006) 1750–1760.
[16] G.Y. Lv, D.J. Sun, J.W. Zhang, et al., Acta Pharm. Sin. B 7 (2017) 52–58.